Available online at www.sciencedirect.com
ScienceDirect
Journal of the European Ceramic Society 30 (2010) 649–656
www.elsevier.com/locate/jeurceramsoc

Sintering, microstructure and mechanical properties of Al_2O_3–Y_2O_3–ZrO_2 (AYZ) eutectic composition ceramic microcomposites

C. Oelgardt [a,*], J. Anderson [b], J.G. Heinrich [a], G.L. Messing [b]

[a] *Department for Engineering Ceramics, Institute of Nonmetallic Materials, Clausthal University of Technology, 38678 Clausthal-Zellerfeld, Germany*
[b] *Department of Materials Science and Engineering, The Pennsylvania State University, University Park, PA 16802, USA*

Received 3 April 2009; received in revised form 11 August 2009; accepted 10 September 2009
Available online 14 October 2009

Abstract

We report on how the mechanical properties of sintered ceramics (i.e., a random mixture of equiaxed grains) with the Al_2O_3–Y_2O_3–ZrO_2 eutectic composition compare with those of rapidly or directionally solidified Al_2O_3–Y_2O_3–ZrO_2 eutectic melts. Ceramic microcomposites with the Al_2O_3–Y_2O_3–ZrO_2 eutectic composition were fabricated by sintering in air at 1400–1500 °C, or hot pressing at 1300–1400 °C. Fully dense, three phase composites of Al_2O_3, Y_2O_3-stabilized ZrO_2 and YAG with grain sizes ranging from 0.4 to 0.8 μm were obtained. The grain size of the three phases was controlled by the size of the initial powders. Annealing at 1500 °C for 96 h resulted in grain sizes of 0.5–1.8 μm. The finest scale microcomposite had a maximum hardness of 19 GPa and a four-point bend strength of 282 MPa. The fracture toughness, as determined by Vickers indentation and indented four-point bending methods, ranged from 2.3 to 4.7 MPa $m^{1/2}$. Although strengths and fracture toughnesses are lower than some directionally or rapidly solidified eutectic composites, the intergranular fracture patterns in the sintered ceramic suggest that ceramic microcomposites have the potential to be tailored to yield stronger, tougher composites that may be comparable with melt solidified eutectic composites.

Keywords: Sintering; Microstructure-final; Mechanical properties; Al_2O_3–Y_2O_3–ZrO_2; Eutectic ceramics

1. Introduction

There is much interest in the mechanical properties of Al_2O_3/($Y_3Al_5O_{12}$) YAG, (Y_2O_3-stabilized ZrO_2) YSZ/YAG, Al_2O_3/ZrO_2 and Al_2O_3–Y_2O_3–ZrO_2 ternary eutectic composites formed by melt quenching,[1–6] rapid solidification[7,8] and directional solidification.[9–13] Some of these materials have impressive high temperature mechanical properties. The distinctive properties of directionally solidified ceramics (DSC) are strength and creep resistance. Directionally solidified Al_2O_3–YAG–YSZ has been reported to have strengths up to 4.6 GPa.[11] A fracture toughness of 9.0 MPa$\sqrt{m}$ was reported for melt quenched Al_2O_3–Y_2O_3–ZrO_2.[2] The distinctive properties of DSC and rapidly quenched ceramics (RQC) are attributed to the lamellar microstructures obtained by the sharp or directional cooling gradients during solidification.

Eutectic defines a composition on the phase diagram that forms a lower temperature liquid between two or more components that co-currently solidify into two or more solid phases when cooled below the eutectic temperature. If a eutectic melt is rapidly or directionally cooled then interesting lamellar phase patterns form upon solidification. For example, solidification of an Al_2O_3–Y_2O_3–ZrO_2 eutectic melt yields a periodic structure with alternating lamellae of alumina and YAG and a Y-stabilized cubic ZrO_2 intermediate phase. The phase spacing decreases to the sub-micron range at the fastest solidification rates.[1,11]

LLorca and Orera noted that directionally solidified ceramic composites are limited in size because melts of small dimensions are required to achieve the thermal gradient and growth rate conditions necessary to obtain a fine lamellar scale.[13] Interestingly, ceramics with the Al_2O_3–Y_2O_3–ZrO_2 eutectic composition have not been fabricated. Sintered composites are of interest because of the relatively lower process costs and the ease of producing large components.[14,15] However, the microstructures in such systems are a composite of equiaxed grains that are randomly and uniformly distributed. In this paper we are interested in determining how the mechanical properties of sintered

* Corresponding author. Tel.: +49 5323 722049; fax: +49 5323 723119.
E-mail address: carina.oelgardt@tu-clausthal.de (C. Oelgardt).

0955-2219/$ – see front matter © 2009 Elsevier Ltd. All rights reserved.
doi:10.1016/j.jeurceramsoc.2009.09.011

ceramics (i.e., a random mixture of equiaxed grains) of the eutectic Al_2O_3–Y_2O_3–ZrO_2 composition compare with those of the rapidly, or directionally solidified Al_2O_3–Y_2O_3–ZrO_2 eutectic melts.

We note that there are a number of reports about the fabrication of dense ceramics based on compositions in the Al_2O_3–Y_2O_3–ZrO_2 system but none with the AYZ eutectic composition.[14,16–19] For example, fracture toughnesses between 4.5 and 5 MPa$\sqrt{}$m were reported for Al_2O_3/YAG ceramics with 5 and 25 vol% YAG.[17,18] A fracture toughness greater than 12 MPa$\sqrt{}$m was reported for Al_2O_3–ZrO_2 composites.[20] The hardness of Al_2O_3–YAG, Al_2O_3–ZrO_2, and Al_2O_3–Y_2O_3–ZrO_2 composites ranges between 14 and 20 GPa.[14,16,18]

To make a valid comparison with the RQ and DS ceramics, we determined how the powder composition affects the sintering process and the scale of the phases formed in this system. Indentation hardness, fracture toughness and fracture strength of the densest composites were measured and compared to the reported properties of melt solidified composites of the same composition.

2. Experimental procedure

The starting materials were 170 nm Al_2O_3 (Taimei Chemicals Co., Ltd., Nagano, Japan), spray-dried 80 nm 3 mol% Y_2O_3-stabilized ZrO_2 (Tosoh Corporation; 3 mol% Yttria, Tokyo, Japan), 60 nm Y_2O_3 (Shin-Etsu Chemical Co., Ltd., Tokyo, Japan) and 300 nm YAG (Nanostructured & Amorphous Materials, Houston, USA). The spray-dried zirconia powder was ball-milled in ethanol for 24 h to break down the agglomerated particles, followed by adding the other powders and then ball-milling for 24 h in ethanol. The milling media were zirconia balls of 3 and 5 mm diameter. The ethanol was removed at 200 °C and the powders were dried at 130 °C. One powder mixture, AYZ, consisted of alumina, yttria and zirconia powders with the ternary eutectic composition (mol%) 65:16:19.[21] A second mixture, YAG-AZ, was prepared by replacing the yttria powder with a YAG powder to determine how 'prereaction' of the YAG phase influences microstructure evolution, sintering behavior and mechanical properties. The initial powder composition of YAG-AZ was 56.38:15.69:27.93 (mol%), which is equivalent to the ternary eutectic composition of the AYZ system after sintering. The two powder mixtures were uniaxially pressed at 4.0 MPa followed by cold isostatic pressing at 200 MPa to obtain 14 mm diameter pellets of 2.5 mm height. After pressing, the pellets were sintered in air at 10 °C/min to 1000 °C, 5 °C/min to the final temperature to 1400, 1450 and 1500 °C, and then cooled at 10 °C/min to room temperature. The sintering times were between 1 and 16 h. Some samples were hot pressed between 1300 and 1400 °C for 0.5–4 h at 18 MPa to achieve smaller grain sizes whereas annealing at 1500 °C for up to 96 h was used to obtain samples with larger grain sizes.

The densities of the sintered samples were determined by the Archimedes technique. The phase composition of the samples was quantified by Rietveld refinement and X-ray diffraction. X-ray diffraction patterns were obtained with a continuous scan of 2° per min (Scintag X2 theta-theta powder diffractometer). A Siemens D500 diffractometer fitted with a Cu tube operating at 40 kV, 30 mA was used to obtain data for the Rietveld refinement over the 10–70° 2θ with a step size of 0.02° and a counting time of 1.5 s at each step. The sintered samples were polished to 1 μm and thermally etched at 100 °C below the sintering temperature to analyse the microstructure by SEM (XL 20, XL Series, Philips). The average grain size was calculated by multiplying the average linear intercept by 1.5.

The hardness was determined by Vickers indentation on polished surfaces (Leco, Model V-100-C1). Vickers hardness was determined from a minimum of 10 indents using a load of 2.9 N. The hardness H was calculated with Eq. (1),[22]

$$H = \frac{P}{2 \cdot a^2} \tag{1}$$

and the fracture toughness K_{IC} was calculated with Eq. (2),[22]

$$K_{IC} = 0.016\left(\frac{E}{H}\right)^{1/2} \frac{P}{c_0^{3/2}} \tag{2}$$

as well as with Eq. (3),[23]

$$K_{IC} = 0.035\left(\frac{H}{E}\right)^{-2/5} \left(\frac{c}{a} - 1\right)^{-1/2} H\sqrt{a}\Phi^{-3/5} \tag{3}$$

where P is the load, a is the half-length of the diagonal, E is the Young's modulus of the material, c_0 is the crack length measured from the middle of the indent to the tip of the crack and Φ is a constraint factor. The Young's modulus was determined by sound velocity to be 330 GPa.

Strength and fracture toughness were also determined by four-point bending. Pellets with a diameter of 38 mm were produced by uniaxial and cold isostatic pressing with the conditions mentioned above and sintered at 1500 °C for 1 h. The sintered pellets were ground flat on one side and polished to 1 micron. The opposing face of the polished side of the pellet was ground to obtain the height of 1.5 mm using a 240 grit diamond polishing wheel. The polished and ground disk was cut into rectangular bars with a width of 2.0 mm. Bars were cut from the center of each disk with final dimensions of 1.5 mm by 2.0 mm by 25 mm. The polished edges of the bend bars were beveled with a 600 grit diamond grinding wheel to limit failure due to edge flaws. Some bend bars were indented in the center of the sample on the polished face using the Vickers hardness tester (Leco, Model V-100-C1) at loads of 4.9, 9.8 and 19.6 N. A drop of oil was pipetted into the crack to prevent further slow crack growth. The fracture toughness K_{IC} was calculated with Eq. (4):[24,25]

$$K_{IC} = 0.59\left(\frac{E}{H}\right)^{1/8} (\sigma_f P^{1/3})^{3/4} \tag{4}$$

where P is the load, H the hardness and σ_f the strength. The Young's modulus E was determined by sound velocity to be 330 GPa.

The four-point bend strength was measured for at least 12 samples at a loading speed of 0.5 mm/min and with a 1 kN load cell (Instron, Model 4202). The outer and inner spans were 20

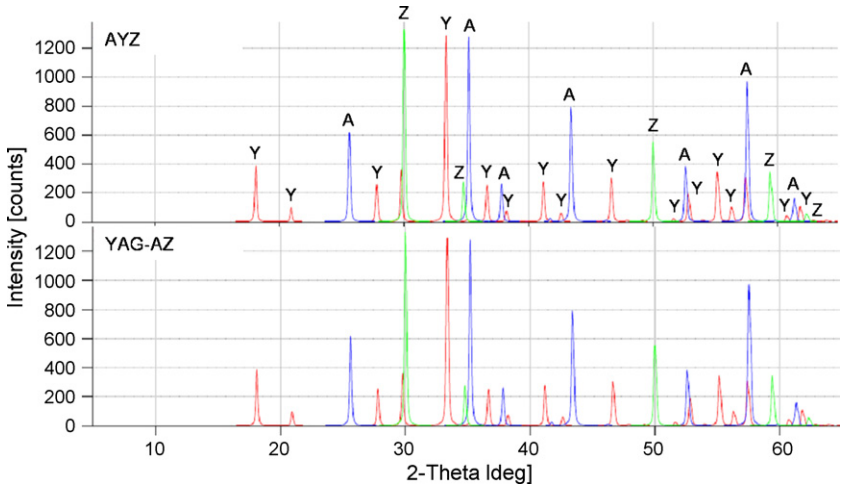

Fig. 1. X-ray diffraction pattern of AYZ and YAG-AZ samples sintered for 1 h at 1400 °C (Y = YAG, A = Al_2O_3, Z = YSZ).

and 10 mm. The strength σ_f was calculated with Eq. (5)[24]:

$$\sigma_f = \frac{3P_f(S_o - S_i)}{2bh^2} \quad (5)$$

where P_f is the fracture load, S_o and S_i are the outer and inner span lengths, b is the thickness, and h is the height.

3. Results and discussion

3.1. Phase composition of the sintered samples

Fig. 1 shows the XRD patterns of the AYZ and YAG-AZ samples sintered at 1400 °C for 1 h. The phase compositions are seen to be nearly identical and thus independent of the source powders. From the Rietveld refinement the samples consist of 45 vol% Al_2O_3, 38 vol% YAG and 17 vol% YSZ for the AYZ system and 43 vol% Al_2O_3, 39 vol% YAG and 18 vol% YSZ for the YAG-AZ system. The zirconia phase after sintering was tetragonal. The theoretical densities of the AYZ and YAG-AZ sintered samples were calculated from the phase composition to be 4.55 and 4.56 g/cm^3, respectively.

3.2. Sintering

Fig. 2 shows the change in sintered density as a function of sintering temperature and time for the two composite systems. The AYZ sample reached full density after 1 h at 1500 °C whereas the YAG-AZ sample reached full density after 2 h. Neither the AYZ nor the YAG-AZ samples reached full density at either 1400 or 1450 °C after 16 h. Except for the slightly higher density of the AYZ system sintered at 1500 °C for 1 h the different starting powder systems had little effect on sintering behavior.

Zhang et al. investigated the pressureless sintering behavior of the nanocrystalline Al_2O_3–Y_2O_3–ZrO_2 system with YSZ (3 mol%) as a function of alumina content from 5 up to 30 mol%.[14] They reported fully dense pellets after sintering for 4 h at 1200 °C with the alumina-free yttria-stabilized sample. The particle sizes of their starting material were around 10 nm. An addition of 5 mol% alumina resulted in a density of 99% whereas an addition of 30 mol% Al_2O_3 lowered the density to 80%. They concluded that alumina suppressed densification and inhibited grain growth. Similar results were reported by Srdić et al.[26] The higher sintering temperature required in our study is most likely due to the higher alumina content in the samples and the larger particle sizes of the initial powders. Fully dense samples were obtained by hot pressing for 30 min at 1400 °C or 2 h at 1350 °C.

3.3. Microstructure and grain growth

The sintered microstructures consisted of zirconia (bright), YAG (gray) and alumina (black) grains (Fig. 3). The sintering behavior of the two powder systems was nearly the same, except for the slight difference after 1 h sintering time. The grain sizes after 1 h sintering time were 0.55 μm for alumina, 0.56 μm for YAG and 0.46 μm for YSZ. The grain sizes in the YAG-AZ system were 0.64 μm for alumina, 0.78 μm for YAG and 0.50 μm for YSZ.

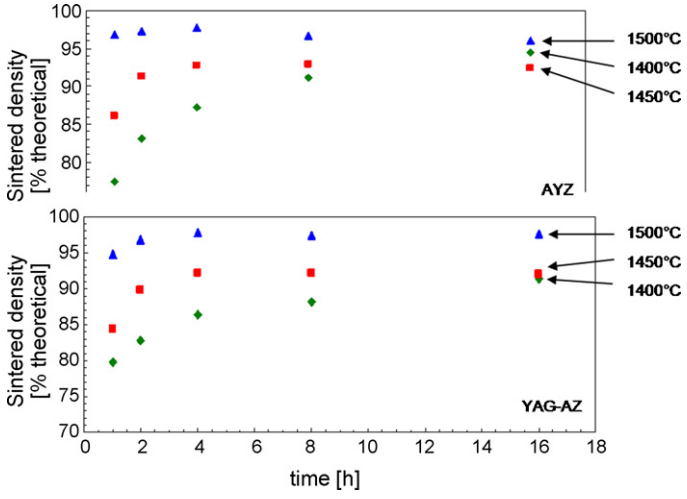

Fig. 2. Sintered density of AYZ and YAG-AZ as a function of sintering time and temperature.

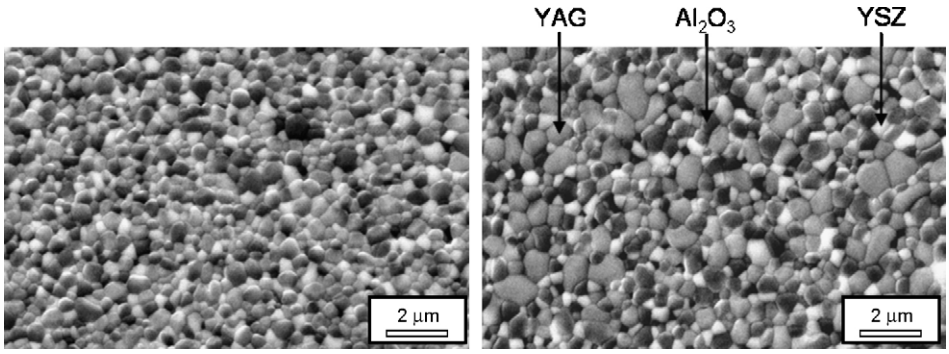

Fig. 3. Microstructure of the sintered microcomposites at 1500 °C for 1 h (polished and thermally etched, SEM, SE); left: starting material AYZ; right: starting material YAG-AZ.

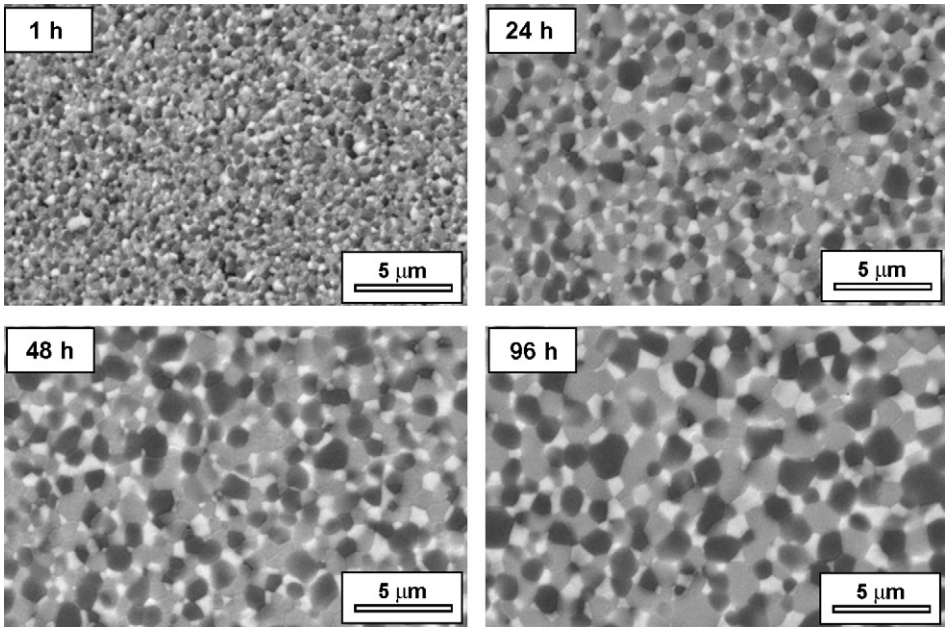

Fig. 4. AYZ samples sintered at 1500 °C up to 96 h (polished and thermally etched, SEM, SE).

Because we could achieve a slightly finer microstructure with the AYZ system, only this system was studied further. The finer microstructure in AYZ could be a result of the smaller yttria particle size compared to the YAG powder used in YAG-AZ. The microstructures and grain sizes of the AYZ system hot pressed for 30 min at 1400 °C are the same as obtained by sintering at 1500 °C for 1 h. The scale of these microstructures is similar to those obtained by rapid solidification from the melt. Also, the microcomposites consist of various two-phase interfaces. In contrast with melt quenched eutectics the interfaces are randomly distributed rather than lamellar.

Grain growth in AYZ samples annealed for 1–96 h at 1500 °C is shown in Fig. 4. The grain sizes started at around 0.5 µm after 1 h and increased to ~1.8 µm after 96 h (Fig. 5). The microstructures are quite stable up to 25 h with alumina coarsening the most to 1.8 µm after 96 h and YSZ coarsening the least to 1.1 µm.

3.4. Mechanical properties

Fig. 6 shows the hardness of the microcomposites as a function of alumina grain size. For comparison we also plot properties of pure YAG, Al_2O_3 and two values for directionally and rapidly solidified AYZ (see also Table 1). Hardnesses of our samples were between 16 and 19 GPa. There is a slight increase in hardness with decreasing grain size. The grain size dependence of the hardness was independent of whether the samples

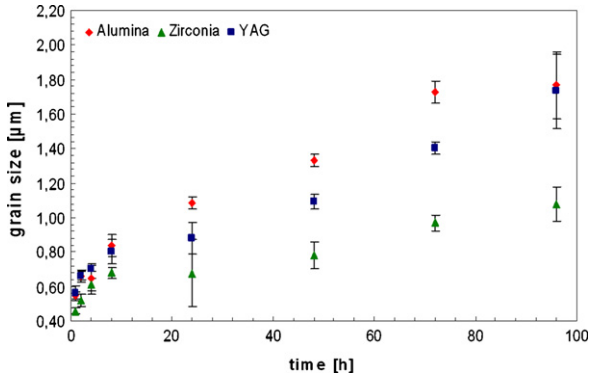

Fig. 5. Grain sizes as a function of the sintering time with a sintering temperature of 1500 °C.

Table 1
Mechanical properties of solidified AYZ ceramics.

Method	Size of the lamellar [μm]	Hardness [GPa]	Fracture toughness [MPa m$^{1/2}$]	Strength [GPa]
Laser-heated floating zone (Peña et al.[12])	~0.7	~15	~3	2.2
Micro-pulling (Lee et a1.[29])	~1.7	15	–	–
Micro-pulling (Lee et a1.[29])	~0.2	17.4	–	1.1 (tensile strength)
Laser zone remelting (Su et al.[8])	~0.15	16.7	8	–
Laser-heated floating zone (grown in nitrogen) (Oliete et. al.[11])	~0.1	–	4.7	4.6
Melt quenching (Calderón-Moreno et. al.[2])	~0.1	–	9	–

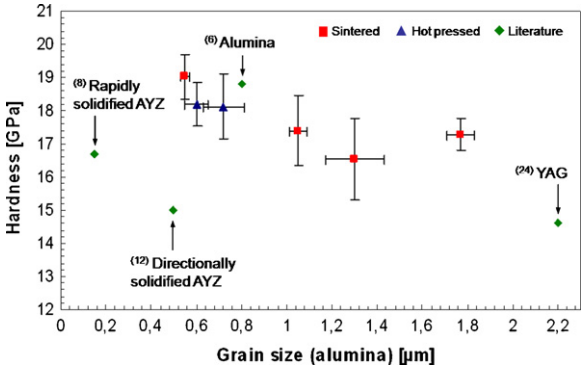

Fig. 6. Hardness of dense AYZ microcomposites as a function of the alumina grain size in comparison with literature data.

were sintered or hot pressed. The hardness was comparable to Al_2O_3 ceramics and considerably higher than YAG ceramic or the melt synthesized AYZ.

Different research groups have tried to improve the mechanical properties of the melt grown binary eutectic ceramics by changing the microstructure with third phase additions or by varying the solidification rate.[27] The hardness of solidified ceramics is mainly dominated by the hardness of the individual phases, especially of the alumina phase.[9,13] Hardness of alumina is influenced by the grain size[6,28] and ranges between 17 and 20 GPa (18.8 GPa for 0.8 μm grain size alumina[6]). Maximum hardnesses reported for directionally solidified Al_2O_3/YSZ binary eutectics range between 18 and 20 GPa and between 13 and 16 GPa for Al_2O_3/YAG binary eutectics.[13] Lee et al. investigated the mechanical properties of ternary eutectic fibers produced by micro-pulling and found an increase in the hardness of up to 17.4 GPa with increasing pulling rate and subsequently decreasing interlamellar spacing.[29] Su et al. produced the ternary eutectic system by rapid solidification with a resulting hardness of 16.7 GPa.[8] The hardnesses obtained with our samples agree with the assertion of Larrea et al.[9] that the alumina phase dominates the hardness of the ceramic composite. It is clear that the microstructure obtained by the melt solidification methods does not yield higher hardnesses and, in fact, was lower than the powder processed ceramics as a result of the finer Al_2O_3 in the RSC.

The strength of directionally solidified eutectics as measured by three-point bending are impressive. Peña et al. reported an average value of 2.2 GPa at ambient temperatures for the ternary eutectic system produced with a solidification rate of 300 mm/h.[12] By using a higher cooling rates (1200 mm/h) nanofibrillar ternary eutectics with spacings of about 100 nm were obtained in nitrogen atmosphere.[11] By reducing the interlamellar spacing the strength increased to 4.6 GPa.

For the sintered composites the four-point-bending strength was 282 ± 49 MPa. The lower strength of the sintered composites is caused by residual porosity and flaws in the ceramic microstructure. As shown for many high performance ceramics, the strength of the sintered ceramic can be increased by decreasing the porosity and processing related flaws. In contrast solidification in nitrogen atmosphere leads to a nearly defect-free microstructure and hence to extremely high mechanical properties.[11]

The determination of the fracture toughness of melt grown and directionally solidified eutectic ceramics and possibilities for increasing this property are points of current interest today. Methods for determining the fracture toughness have been sharply criticized recently.[30] Nevertheless, the determination of fracture toughness by the Vickers indentation fracture test (VIF) is very popular because of the ease of sample preparation and testing.

Many researchers in the field of directionally solidified and melt quenched eutectic ceramics used the VIF method for the estimation of the fracture toughness. The main reason may be that only small sample sizes can be produced at the high cooling rates required to obtain lamellar microstructures. For comparison we also used the VIF to determine K_{IC}. For the indentation method it is critical to use the correct equation for the K_{IC} calculation. The crack geometries which can be formed are Palmqvist cracks or median cracks as well as a mixture of both. For median cracks, where the ratio between crack length and indent diagonal is $c/a \geq 2.5$, the equation by Anstis et al. (Eq. (2))[22,9] is used. For Palmqvist cracks, i.e., $c/a < 2.5$, the equation by Niihara (Eq. (3))

Table 2
Ratio of crack length and half-diagonal of dense samples.

Sintering condition	Crack length c [μm]	Diagonal half-length a [μm]	c/a
Sintered			
1500 °C, 1 h	39.3 ± 5.0	16.4 ± 0.1	2.4 ± 0.3
1500 °C, 24 h	38.3 ± 4.4	16.8 ± 0.2	2.3 ± 0.3
1500 °C, 96 h	41.6 ± 4.9	17.1 ± 0.4	2.4 ± 0.3
1650 °C, 48 h	39.4 ± 6.7	17.1 ± 0.5	2.3 ± 0.4
Hot pressed			
1400 °C, 0.5 h	34.6 ± 5.1	16.5 ± 0.4	2.1 ± 0.3
1400 °C, 2 h	31.6 ± 5.0	16.5 ± 0.6	1.9 ± 0.3

Table 3
Fracture toughness of dense samples.

Sintering condition	Alumina grain size [μm]	Median crack [MPa m$^{1/2}$]	Palmqvist crack [MPa m$^{1/2}$]	4-Bending method [MPa m$^{1/2}$]
Sintered				
1500 °C, 1 h	0.55	2.7 ± 0.5	3.8 ± 0.4	2.3 ± 0.2
1500 °C, 24 h	1.05	3.0 ± 0.5	3.9 ± 0.4	–
1500 °C, 96 h	1.77	2.6 ± 0.4	3.6 ± 0.4	–
1650 °C, 48 h	2.45	3.0 ± 0.8	3.7 ± 0.7	–
Hot pressed				
1400 °C, 0.5 h	0.60	–	4.2 ± 0.6	–
1400 °C, 2 h	0.72	–	4.7 ± 0.9	–

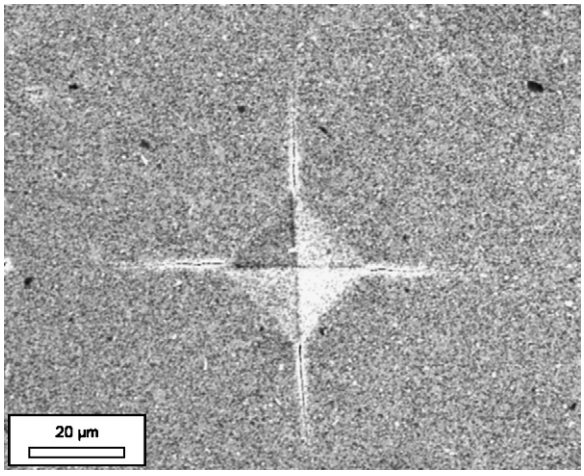

Fig. 7. Vickers indentation with cracks in the sintered AYZ sample (polished, SEM, SE).

is used.[23,9] The indentation results for the sintered samples are listed in Table 2 (mean values of at least 10 indents). It is important to note that – considering the standard deviations of the indent dimensions – the ratio of crack length and indent diagonal is at the limit between which equation to use to calculate K_{IC}. Only the hot pressed samples fall unequivocally below a c/a of 2.5 and thus Eq. (3) was used to calculate K_{IC} of these samples. The classification of the other samples to one crack type or the other is difficult, therefore both equations were used to compare the results (Table 3). We see that the samples range from 2.7 to 3.0 MPa$\sqrt{}$m and 3.6 to 3.9 MPa$\sqrt{}$m if we assume median and Palmquist cracks, respectively. The hot pressed samples, which were denser than the sintered samples, had toughnesses of 4.2 and 4.7 MPa$\sqrt{}$m. It is interesting that there does not appear to be any grain size effect on the fracture toughness. Unfortunately, we do not have bend bars of the hot pressed samples for testing.

The fracture toughness for the sintered composite was also measured by four-point bending with three different indentation loads. The resulting fracture toughness was independent of load and determined to be 2.3 ± 0.2 MPa$\sqrt{}$m (see also Table 3). This fracture toughness is comparable with the result from the VIF method, calculated with the Eq. (2) for median cracks.

In the case of DSC and RQC, the only binary eutectics in Al_2O_3/YAG were reported to have median cracks, otherwise the equation for Palmqvist cracks is widely used. LLorca et al. reported fracture toughnesses between 4 and 5 MPa$\sqrt{}$m for the binary eutectic Al_2O_3/YSZ and values of around 2 MPa$\sqrt{}$m for the binary eutectic Al_2O_3/YAG.[13] Peña et al. achieved fracture toughnesses of 4.3 MPa$\sqrt{}$m for the ternary eutectic system Al_2O_3/YAG/ZrO_2.[12] Unusually high fracture toughnesses were reported by Calderon-Moreno et al. for rapidly quenched Al_2O_3/YAG/ZrO_2 ternary eutectic[2] that had phase spacings of ∼100 nm. They reported a fracture toughness of around 9.0 MPa$\sqrt{}$m.[2] Unfortunately, there exist no micrographs from Calderon-Moreno et al. which show the crack path in the melt quenched samples to explain the outstanding fracture toughness values. Su et al. reported 8.0 MPa$\sqrt{}$m for rapidly solidified Al_2O_3/YAG/ZrO_2 eutectic with phase spacings of about 150 nm.[8] Both groups explain the high fracture tough-

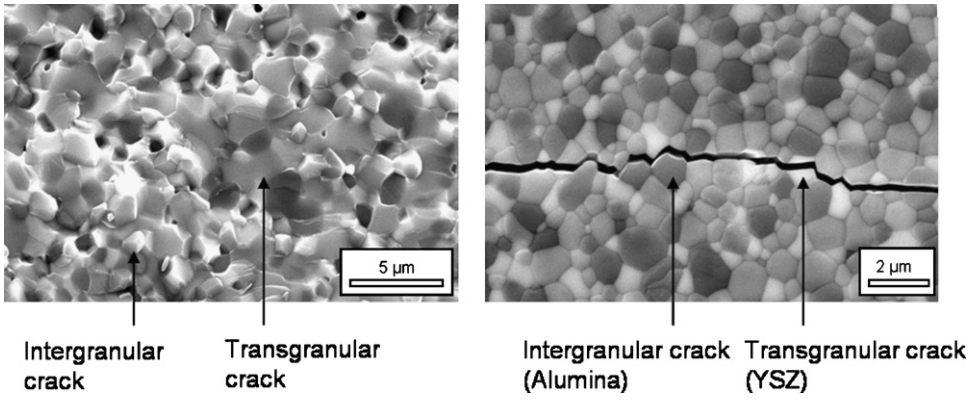

Fig. 8. Crack path in the AYZ microcomposite; left: fracture surface (SEM, SE); right: surface with cracks (polished, thermally etched, SEM, SE).

ness, which is twice as high as the fracture toughness published for DSCs, by a stronger interaction between the crack and the eutectic interphases caused by the refinement of the eutectic microstructure. The stronger interaction can induce crack deflection and branching which results in an increase of the fracture toughness.[2,8]

In contrast with the above findings, Peña et al. found higher fracture toughness values for ternary eutectics with a coarser microstructure produced with a slower solidification rate (10 mm/h) than 1000 mm/h.[12] They observed stronger crack deflection and branching with larger domain sizes. More work is needed or more data should be reported to verify or justify these properties.

Fig. 7 shows an SEM micrograph of the Vickers indent with cracks in the microstructure and Fig. 8 shows the crack path in the AYZ microcomposite. Transgranular as well as intergranular cracks were observed. This suggests that the microstructure and scale can be tailored to yield better mechanical properties.

4. Conclusion

Dense ceramics with the ternary eutectic composition in the Al_2O_3–Y_2O_3–ZrO_2 system were obtained by sintering in air and hot pressing. The phases developed after sintering were Al_2O_3, Y_2O_3-stabilized tetragonal zirconia and YAG. The results showed that the starting powder composition did not influence the sintering behavior and the properties, so it is not critical whether one uses Y_2O_3 or YAG as the starting material, at least for the thermal conditions of this study. Sintering temperature seems to influence the yttria content in the zirconia solid solution but more work is necessary for a better understanding of the processes during sintering in the ternary system.

Hardness of the samples, measured by the Vickers indentation method, showed maximum values of 19 GPa. The bending strength of sample sintered for 1 h at 1500 °C was 282 MPa. It is important to note that a low sintering temperature resulted in dense and fine grain size microstructure after starting with simply processed powders and pressureless sintering.

Fracture toughness was determined by Vickers indentation method as well as by four-point bending. The *c*/*a* ratio for indents in microcomposites was sufficiently different from 2.5 to assume either median or Palmqvist cracks. Assuming median cracks, a more conservative estimate of fracture toughness was 2.6–3.0 $MPa\sqrt{m}$ with the VIF method which agreed with the 2.3 $MPa\sqrt{m}$ obtained with the bending method. The hot pressed samples, which had a lower porosity than the sintered samples, had fracture toughnesses of 4.2 and 4.7 $MPa\sqrt{m}$. These values are comparable to some of the literature reports for two-phase composites in the Al_2O_3–Y_2O_3–ZrO_2 system.

References

1. Calderon-Moreno, J. M. and Yoshimura, M., Microstructure and mechanical properties of quasi-eutectic Al_2O_3–$Y_3Al_5O_{12}$–ZrO_2 ternary composites rapidly solidified from melt. *Mater. Sci. Eng. A*, 2004, **375–377**, 1246–1249.
2. Calderon-Moreno, J. M. and Yoshimura, M., Al_2O_3–$Y_3Al_5O_{12}$(YAG)–ZrO_2 ternary composite rapidly solidified from the eutectic melt. *J. Eur. Ceram. Soc.*, 2005, **25**, 1365–1368.
3. Calderon-Moreno, J. M. and Yoshimura, M., Effect of melt quenching on the subsolidus equilibria in the ternary system Al_2O_3–$Y_3Al_5O_{12}$–ZrO_2. *Solid State Ionics*, 2001, **141/142**, 343–349.
4. Calderon-Moreno, J. M. and Yoshimura, M., $Y_3Al_5O_{12}$(YAG)–ZrO_2 binary eutectic composites obtained by melt quenching. *Mater. Sci. Eng. A*, 2004, **375–377**, 1250–1254.
5. Calderon-Moreno, J. M. and Yoshimura, M., Nanocomposites from melt in the system Al_2O_3–YAG–ZrO_2. *Scr. Mater.*, 2001, **44**, 2153–2156.
6. Rosenflanz, A., Frey, M., Anderson, T. and Richards, E., Bulk glasses and ultrahard nanoceramics based on alumina and rare-earth oxides. *Nature*, 2004, **430**, 761–764.
7. Su, H., Zhang, J., Cui, C., Liu, L. and Fu, H., Rapid solidification behaviour of Al_2O_3/$Y_3Al_5O_{12}$ (YAG) binary eutectic ceramic *in situ* composites. *Mater. Sci. Eng. A*, 2008, **479**, 380–388.
8. Su, H., Zhang, J., Cui, C., Liu, L. and Fu, H., Rapid solidification of Al_2O_3/$Y_3Al_5O_{12}$/ZrO_2 eutectic in situ composites by laser zone remelting. *J. Cryst. Growth*, 2007, **307**, 448–456.
9. Larrea, A., Orera, V. M., Merino, R. I. and Peña, J. I., Microstructure and mechanical properties of Al_2O_3–YSZ and Al_2O_3–YAG directionally solidified eutectic plates. *J. Eur. Ceram. Soc.*, 2005, **25**, 1419–1429.
10. Larrea, A., de la Fuente, G. F., Merino, R. I. and Orera, V. M., ZrO_2–Al_2O_3 eutectic plates produced by laser zone melting. *J. Eur. Ceram. Soc.*, 2002, **22**, 191–198.
11. Oliete, P. B., Peña, J. I., Larrea, A., Orera, V. M., LLorca, J., Pastor, J. Y. *et al.*, Ultra-high-strength nanofibrillar Al_2O_3–YAG–YSZ eutectics. *Adv. Mater.*, 2007, **19**, 2313–2318.
12. Peña, J. I., Larsson, M., Merino, R. I., de Francisco, I., Orera, V. M., LLorca, J. *et al.*, Processing, microstructure and mechanical properties of directionally-solidified Al_2O_3–$Y_3Al_5O_{12}$–ZrO_2 ternary eutectics. *J. Eur. Ceram. Soc.*, 2006, **26**, 3113–3121.
13. LLorca, J. and Orera, V. M., Directionally solidified eutectic ceramic oxides. *Prog. Mater. Sci.*, 2006, **51**, 711–809.
14. Zhang, Y., Chen, J., Hu, L. and Liu, W., Pressureless-sintering behavior of nanocrystalline ZrO_2–Y_2O_3–Al_2O_3 system. *Mater. Lett.*, 2006, **60**, 2302–2305.
15. Zhang, S. C., Hilmas, G. E. and Fahrenholtz, W. G., Pressureless sintering of ZrB_2–SiC ceramics. *J. Am. Ceram. Soc.*, 2008, **91**, 26–32.
16. Ye, Y., Li, J., Zhou, H. and Chen, J., Microstructure and mechanical properties of yttria-stabilized ZrO_2/Al_2O_3 nanocomposite ceramics. *Ceram. Int.*, 2008, **34**, 1797–1803.
17. Wang, H., Gao, L., Shen, Z. and Nygren, M., Mechanical properties and microstructure of Al_2O_3–5 vol% YAG composites. *J. Eur. Ceram. Soc.*, 2001, **21**, 779–783.
18. Li, W. Q. and Gao, L., Processing, microstructure and mechanical properties of 25 vol% YAG–Al_2O_3 nanocomposites. *Nanostruct. Mater.*, 1999, **11**, 1073–1080.
19. Wang, H. and Gao, L., Preparation and microstructure of polycrystalline Al_2O_3–YAG ceramics. *Ceram. Int.*, 2001, **27**, 721–723.
20. Wang, J. and Stevens, R., Review zirconia-toughened alumina (ZTA) ceramics. *J. Mater. Sci.*, 1989, **24**, 3421–3440.
21. Lakiza, S. N., Lopato, L. M., Nazarenko, L. V. and Zaitseva, Z. A., The liquidus surface in the Al_2O_3–ZrO_2–Y_2O_3 phase diagram. *Powder Metall. Met. Ceram.*, 1994, **33**, 595–598.
22. Anstis, G. R., Chantikul, P., Lawn, B. R. and Marshall, D. B., A critical evaluation of indentation techniques for measuring fracture toughness: I. Direct crack measurements. *J. Am. Ceram. Soc.*, 1981, **64**, 533–538.
23. Niihara, K., A fracture mechanics analysis of indentation-induced Palmqvist crack in ceramics. *J. Mater. Sci. Lett.*, 1983, **2**, 221–223.
24. Mezeix, L. and Green, D. J., Comparison of the mechanical properties of single crystal and polycrystalline yttrium aluminium garnet. *Int. J. Appl. Ceram. Technol.*, 2006, **3**, 166–176.
25. Chantikul, P., Anstis, G. R., Lawn, B. R. and Marshall, D. B., A critical evaluation of indentation techniques for measuring fracture toughness: II. Strength method. *J. Am. Ceram. Soc.*, 1981, **64**, 539–543.
26. Srdić, V. V., Winterer, M. and Hahn, H., Sintering behavior of nanocrystalline zirconia doped with alumina prepared by chemical vapor synthesis. *J. Am. Ceram. Soc.*, 2000, **83**, 1853–1860.

27. LLorca, J., Pastor, J. Y. and Poza, P., Influence of the Y_2O_3 content and temperature on the mechanical properties of melt-grown Al_2O_3–ZrO_2 eutectics. *J. Am. Ceram. Soc.*, 2004, **87**, 633–639.
28. Teng, X., Liu, H. and Huang, C., Effect of Al_2O_3 particle size on the mechanical properties of alumina-based ceramics. *Mater. Sci. Eng. A*, 2007, **452/453**, 545–551.
29. Lee, J. H., Yoshikawa, A., Fukuda, T. and Waku, Y., Growth and characterization of $Al_2O_3/Y_3Al_5O_{12}/ZrO_2$ ternary eutectic fibers. *J. Cryst. Growth*, 2001, **231**, 115–120.
30. Quinn, G. D. and Bradt, R. C., On the Vickers indentation fracture toughness test. *J. Am. Ceram. Soc.*, 2007, **90**, 673–680.